

Electrochemical Determination of Hg(II) Ions Based on Biosynthesized Spherical Activated Carbon from Potato Starch

Qiao Lin^{1,2*}, Xu Peng^{1,2} and Zhong Zhang^{1,2}

¹ School of Applied and Chemical Engineering, Xichang College, Xichang, 615000, China

² Demonstration Center for the Engineering of Serving Potatoes as Staple Food, Xichang College, Xichang, 615000, China.

E-mail: 13778673369@163.com

Received: 19 November 2016 / Accepted: 30 December 2016 / Published: 12 February 2017

The method, where carbonization of potato starch with high temperature is followed by hydrothermal process without catalyst, is employed to fabricate the well-defined and individual carbon microspheres (designated as MC). The method, such as FTIR, SEM, BET, Raman and XRD, are used to detect the properties of the synthesized samples. Next, we show that a noble sensor with high sensitivity and selectivity for Hg (II) with a glassy carbon electrode which is decorated by MC, which behaves as platform with enhanced sensing. The processes of transferring the electron and behaviour of detecting the Hg (II) are greatly facilitated by advised sensor, which leads to the sensor more selective and sensitive. The limit of detection is about 5 ppm, which is much lower than that of WHO (which is short for World Health Organization). This method can inhibit the disturbance of the Zn²⁺, Cu²⁺ and Fe³⁺ ions when the mercury is analysed.

Keywords: Electrochemical sensor; Hg ions; Carbon microspheres; Biosynthesis; Photo starch

1. INTRODUCTION

In the fields of the medicine, process control, biology and environmental analysis, there is great interested of determining the trace concentration of ions of heavy metal. Due to its important effect to environment and toxicology, the vestibular dysfunction, speech difficulty, hearing loss, autism, impaired vision and mental deterioration are reported to be the results of neurotoxicity of mercury [1]. The work, determining mercury with low the concentration in different samples, such as water, is essential when the notice of its pollution to environment and toxicity is growing. As we know, WHO set the limit to the drinking water, which is 1 µg/L [2]. Due to its accumulation and persistence in the

biota as well as environment, EPA (which is short for Environmental Protection Agency) also considers about the mercury. Meanwhile, because of negative effect to human beings, the amounts of extremely low concentration mercury has been important in the chemistry of environment and clinic; so, different methods, like ICP mass spectrometry [3], ICP, cold vapor atomic absorption spectroscopy (CVAAS) [4, 5] and analysis of activating the neutron [6] were employed to determine the low concentration of mercury. The majority of the methods are taking lots of time, expensive, invalid for mercury with on-site, where the various manipulations of sample is involved in monitoring of these methods. While, the detection with electrochemistry method provides some advantages, which is cheap, easy, direct, fast and miniaturized [7]. Because of its accuracy, fast response, low cost and non-destruction, the interest of analytical investigation is still involving to develop and apply the electrode with ion selectivity to sensors to cations and anionic of metal species [8-14].

ACs can be used in many applications, meanwhile the noble applications are still coming, and it indicates that the stable increase of ACs consumption is a fact. The morphology of ACs determine their applications, while there are various methods to fabricate different ACs, such as powder ACs (designated as the PACs), GACs (which is short for granular ACs) [15, 16], ACFs (which is short for activated carbon fibers) [17], carbon monoliths and ACs with spherical way [18, 19]. Due to its advantages, which shows wear resistant, strengthen, excellent adsorption, highly pure, surface with smooth issue, content with low ash, excellent fluidity, drop with extremely low pressure, excellent packaging, controlled dispersion ability to pore size, high density under bulk condition and high micropore volume, Spherical ACs has attracting increasing attention compared with granular and powdered ACs [20, 21]. The spherical ACs has been applied to purify the blood, be support of catalysts, act as chemical protection to sensors or clothing, owing to its great advantages [19, 22]. It is also potential to support a lot of processes of absorption, no matter in gas or liquid [23, 24]. Bearing these in mind, a lot of investigation has been performed to fabricate this kind of materials by employing various experimental method. Now, carbon-based materials can be fabricated from plant resources and side-products of agriculture. For example, carbonization of subcritical water was employed to fabricate CMSs (which is short for sugar-derived carbon microspheres), which was reported by Kurniawan et al. [25]. Synthesis of co-doped MCs with nitrogen and phosphorus was reported by Wang's group [26]. Recently, the glucose was employed as a carbon resources to synthesize PCS, which is reported by Wang and co-workers with a mild method of hydrothermal [27]. carbon spheres with micro-mesopore was fabricated by Yang with carrageenan under hydrothermal carbonization [28]. While, potato starch, as a non-cost and polysaccharide with much availability, has not been employed as an environmental carbon precursor to fabricate the MCMS with high dispersion by using hydrothermal method. Here, we report that the high quality CM with high yield is fabricated by an easy and effective hydrothermal method by taking the potato starch as a resource. The absence of chemicals in this preparation method makes it efficient and environment benign. Next, the MC behaviour of electrochemical was investigated. The electrode decorated by MC was employed to determine the Hg(II) ions with electrochemistry. The stability, rapidness and sensitivity of Hg(II) measurements are improved by adding the MC. The investigation of determining the Hg(II) under stripping is performed in the novel platform.

2. EXPERIMENTS

2.1. MC preparation

The mild hydrothermal method was employed to fabricate the CM with high dispersion through carbonization under high temperature with N₂. Typically, potato starch with 2 g of powder was mixed with 100 ml of water (distilled), and the mixture was stirred with 5 hours. After that, the solution was transported into the 150 ml of autoclave with Teflon-lined stainless steel, and another 16 hours was needed for this hydrothermal treatment at 180 °C. Thereafter, the autoclave was cooled to room temperature, where dark precipitates formed. The filtered products were purified by the ethanol and water and dried at 60 °C in a vacuum with 12 hours. The MC-180 was the label of the as-obtained sample. The sample was put into the furnace under a rate of 4 °C/min and treated under N₂ of 10ml/min with 900 °C in 2 hours. This resulted sample was designated as MC-900.

2.2. Characterization techniques

The morphology of all samples was characterized by a Philips XL30 scanning electron microscopy (SEM). N₂ adsorption isotherms were carried out on Micrometrics ASAP3000 adsorption analyser at 77 K. Samples were degassed at 300 °C for 4 h under high vacuum prior to measurement. For electrocatalytic activity test, All electrochemical measurements were performed on a CHI430a electrochemical workstation (USA) at room temperature. A conventional three electrode system containing a modified GCE as working electrode, a platinum wire as auxiliary electrode and a Ag/AgCl (3M KCl) electrode as reference electrode was used throughout the electrochemical experiments. Attenuated total reflectance Fourier transform infrared spectra (ATR-FTIR) spectra were recorded on a Nicolet iS5 (USA) spectrometer. Solid samples were placed on the diamond reflectance area for direct transmittance data collection. The powder X-ray diffraction (XRD) patterns of samples were collected from 5° to 90° in 2θ by an X-ray diffractometer with Cu Kα radiation (D8-Advanced, Bruker, Germany). Raman analysis was carried out at room temperature using a Raman spectroscope (Renishaw InVia, UK) with a 514 nm laser light.

2.3. Stripping voltammetric detection of mercury at MC modified GCE

Before electrochemical measurements, GCE was polished using alumina. The surface modification process contains following procedure: 5 μL of modifier solution (0.5 mg/mL) were dropped on the surface of electrode, and then dried naturally. Square wave anodic stripping voltammetry (SWASV) was utilized to perform the continuous determination of Hg (II) under the optimized conditions. Mercury was deposited at -0.2 V for 120 s in a 1 M HCl solution. The anodic stripping of electrodeposited Hg(0) was performed from 0 to 0.7 V under optimized conditions (frequency, amplitude, potential increment were 40 Hz, , 20 mV, and 4 mV, respectively). For the removal of the deposited mercury, multiple continuing SWASV scanning was employed until no

anodic stripping response was observed. In addition, regeneration of the sensor surface was achieved. Real tap water was used for practical application tests.

3. RESULTS AND DISCUSSION

The morphology of MC-180 and MC-900 were characterized by SEM, and images were demonstrated in Fig. 1A and 1B, respectively. According to the panoramic SEM image shown in Figure 1A, it was obvious that the samples exhibited a massive uniform microspheres with an average size of 300 nm, where no agglomeration was observed. The morphological yield of these microspheres is approximately 40%. In Figure 1B, the CM-900 particles displayed a perfect spherical shape. The average diameter of these particles is 220 nm which is much smaller than that of CM-180. This is probably owing to gasification of carbon at high temperature. Furthermore, CM-900 particles construct a porous structure which can act as an ion buffer “reservoir” for electrolyte, which is favourable for the ion transportation towards the surface of the electrode.

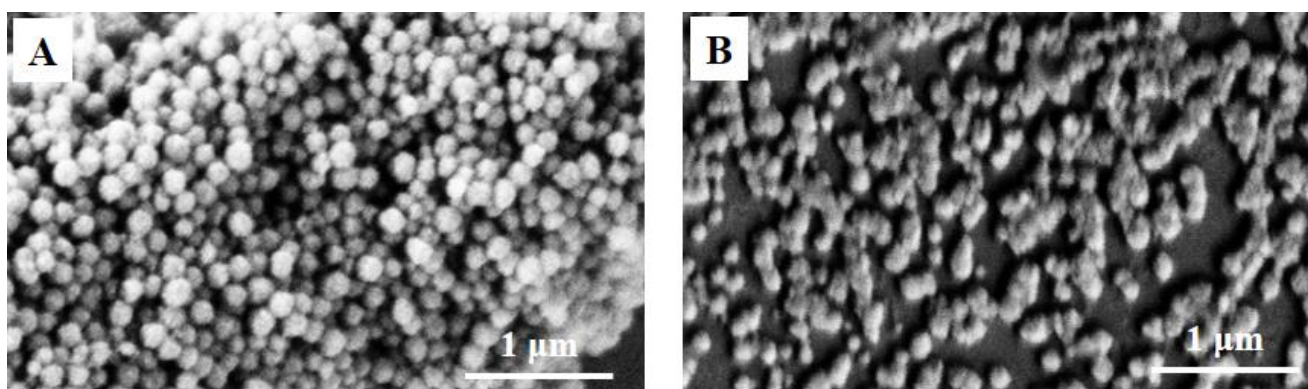


Figure 1. SEM images of MC-180 (A) and MC-900 (B).

The XRD patterns of MC-180 and MC-900 are clarified in Figure 2A. It is obvious that the MC-180 and MC-900 both exhibit a broad diffraction peak located at 22.4° which is attributed to the (002) plane of graphite. Raman spectrum of the MC-900 was illustrated in Fig. 2B, where two strong peaks are observed at 1318 and 1577 cm^{-1} . The peak at 1577 cm^{-1} (G band) is ascribed to a graphite E_{2g} mode which is in a relation to the vibration of sp^2 -bonded carbon atoms in 2D hexagonal lattice of graphite layer. The peak at 1318 cm^{-1} (D band) corresponds to vibrations of carbon atoms with dangling bonds in a disordered termination plane [29, 30]. The intensity ratio of D band to G band (ID/IG), which is determined by the type of graphitic materials, reflects the graphitization level of the carbon materials. The ID/IG ratio of MC-900 is 1.04, whereas the amorphous carbons usually exhibits a ID/IG value of 1.00 [31]. This reveals that the disordered carbon takes place. In addition, the full width at half maximum (FWHM) of the D band is broader compared with that of G band, indicating

the presence of a large proportion of structure defects as well as a disorder state in the obtained carbons [32].

The FTIR of the MC-180 and MC-900 are elaborated in Figure 2C. The bands at 3432 and 1104 cm^{-1} correspond to the hydroxyl or carboxyl stretching vibration and C—OH bending vibration, respectively, indicating that large numbers of —OH groups are present on the MC surface. The peaks at 1618 and 1700 cm^{-1} are ascribed to the bending vibration of O—H in the adsorbed water and the stretching vibration of carbonyl in the carboxyl groups, respectively. This suggests that adsorbed water is present in MC-180. The band from 870 to 755 cm^{-1} is attributed to aromatic C—H out-of-plane bending vibrations, showing the existence of aromatization such as the aldol dehydration and condensation. However, the peak at 1697 cm^{-1} in the FTIR spectrum of MC-900 is not observed, suggesting that the carbonization of MC-900 is more complete than that of MC-180.

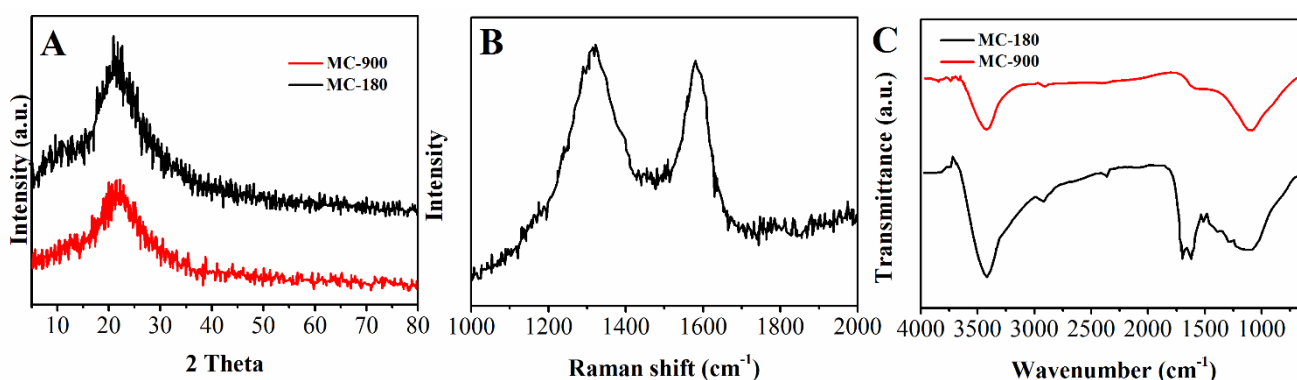


Figure 2. XRD patterns of MC-180 and MC-900 (A), Raman spectrum of MC-900 (B), FTIR spectra of MC-180 and MC-900 (C).

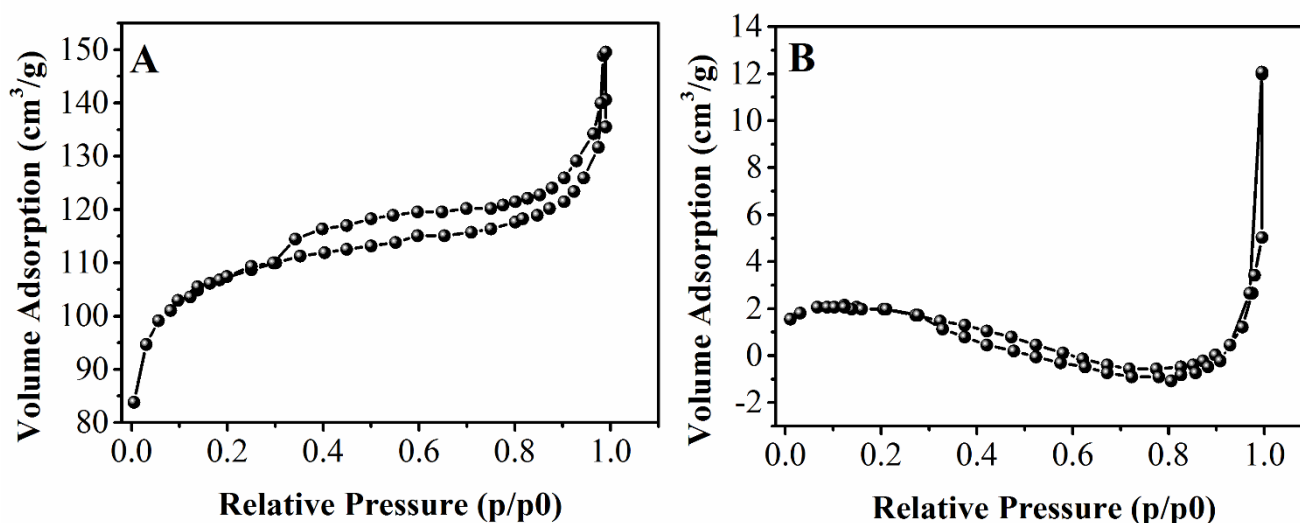


Figure 3. Nitrogen adsorption/desorption isotherms and pore size distributions of MC-900 (A) and MC-180 (B).

N_2 adsorption/desorption isotherms and corresponding pore size distribution of MC-900 were carried out and listed in Fig. 3A. A significant hysteresis loop is observed in the curve of MC-900 in Figure 3A under a relative pressure of P/P_0 ranging from 0.30 to 1.0, which could be recognized as type IV isotherms based on the IUPAC definition, implying a characteristic of mesoporous structure. Besides, the mesoporous MC-900 exhibits a specific surface area of $447 \text{ m}^2/\text{g}$. In the inset of Figure 3A, it is obvious that the pore size distribution curve of as-prepared MC-900 centres at 3.9 nm, as well as a low intensity of width pore size distribution ranges from 10 to 15 nm.

The porosity of the MC-900 is beneficial to the soak of electrolytes into the particles to generate more channels for the transportation of the electrolyte ions. Besides, more electroactive sites could be provided with such porosity for fast energy storage under large current densities. Differently, the specific surface area of MC-180 is only $6.1 \text{ m}^2/\text{g}$ (as shown in Fig. 3B). N_2 adsorption and desorption isotherms of MC-180 which are absence of an obvious hysteresis loop are identified as the type III. There is tiny adsorption can be observed at relatively low pressure suggesting the existence of few microporous. Therefore, the MC-180 has a non-porous surface. Although the pore size distribution curve shows that macropores are present in as-prepared MC-180 (inset of Fig. 3B), this can be ascribed to the slits in MC-180 (obtained in the SEM images).

Fig. 4A depicts the chronocoulometric curves on different electrodes for the reduction of $0.5 \text{ mM K}_3\text{Fe}(\text{CN})_6$ with 0.1 M KCl .

$$Q = (2nFAD_0^{1/2} \pi^{-1/2} C) t^{1/2}$$

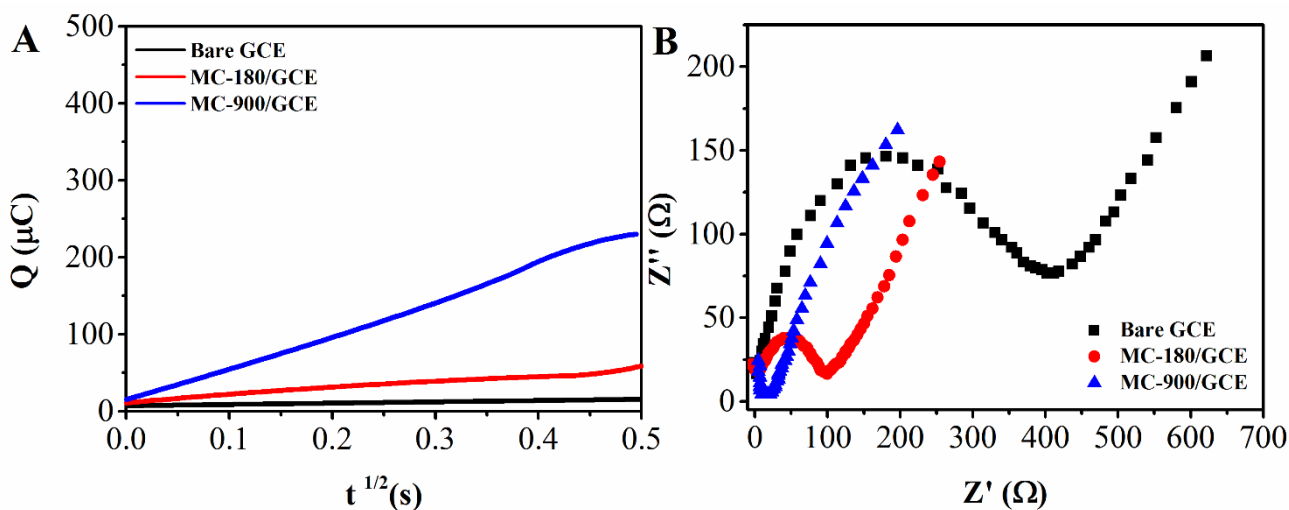


Figure 4. (A) Chronocoulometric curves for the reduction of $\text{K}_3\text{Fe}(\text{CN})_6$ with a concentration of 0.5 mM in the presence of KCl with a concentration of 0.1 M at GCE electrodes, MC-180/GCE and MC-900/GCE, where the potential was 0.65 V at the beginning and then stepped to -0.05 V . (B) Nyquist plots of GCE electrodes, MC-180/GCE and MC-900/GCE in $\text{Fe}(\text{CN})_6^{3-/4-}$ with a concentration of 10 mM in the presence of KCl with a concentration of 0.1 M , where the frequency varied in the range of 1 Hz to 100 kHz .

According to equation described above, the absolute value of the reduction charge is represented by Q , where the number of the electrons in the reaction, the Faraday constant and the

surface area of the electrode are illustrated with n , F and A , respectively. Besides, the diffusion coefficient of the oxidized state of hexacyanoferrate (III), the bulk concentration of the oxidized as well as the time are represented by D_0 , C_0 and t , respectively. Based on the slope of the $Q-t^{1/2}$ line, the order of A of various electrodes is calculated to be bare GCE (curve *a*, 0.105 cm^2) < MC-9180GCE (curve *b*, 0.366 cm^2) > MC-900/GCE (curve *c*, 0.848 cm^2). It demonstrates that the active area of the surface is improved significantly by the modification of GCE with MC-900, which exhibits potential applications in the field of sensing.

In Figure 4B, the electrochemical impedance spectra (EIS) was employed to further investigated the electron transfer performance of diverse electrodes. A semicircle and a straight line were observed in the EIS of the bare GCE, which clarified the diffusion-limiting procedure of the $\text{Fe}(\text{CN})_6^{4-/3-}$ processes. The diameter of the semicircle reduced when modifying the GCE with MC, which was in accordance with the fact that graphene exhibited high electrical conductivity as well as the reduced resistance of charge transfer (R_{ct}). However, the diameter of the semicircles was reduced gradually when changing the modification of GCE with MC-180 to MC-900, compared to the EIS of the bare GCE. This indicated that the heterogeneous electron transfer kinetics exhibited increasingly facile, which demonstrated that MC-900/GCE exhibited a higher electrochemical activity compared to that of GC and MC-180/GCE electrodes.

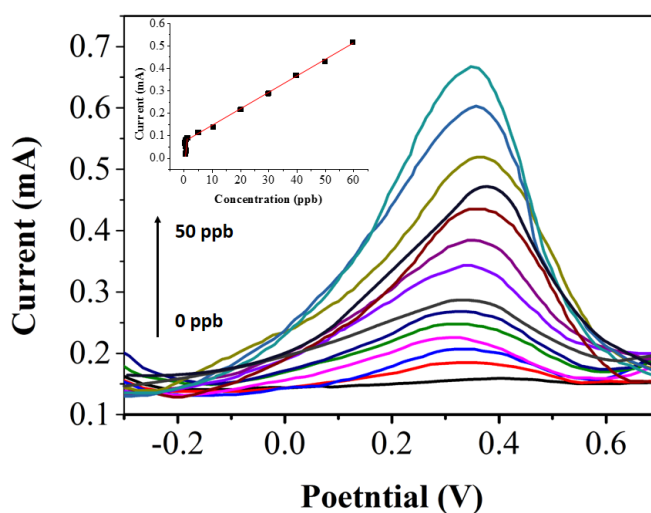


Figure 5. Stripping voltammograms of mercury with varying concentrations of Hg (II) from bottom to top, 0, 0.005, 0.01, 0.03, 0.05, 0.08, 0.1, 0.5, 1.0, 5.0, 10, 20, 30 and 50 ppb, respectively. Conditions: 0.1 M HCl; frequency: 40 Hz; amplitude: 20 Mv; potential increment: 4 mV.

Moreover, the MC-900.GCE was also employed to determine Hg (II) continuously through SWASV. The SWASV responses of MC-900/GCE to Hg (II) with various concentrations in the presence of HCl with a concentration of 1 M was illustrated in Figure 5. The well-defined peaks were observed in the ranges of 0.005 to 0.08 ppb and 0.1 to 50 ppb, where the peaks exhibited a positive relationship with the concentration of Hg (II). Especially, based on the slope of the calibration plot, the sensitivity of the electrode was measured to be $603.2 \mu\text{A/ppb}$ when the concentration of Hg (II) was lower, which was significantly higher compared with methods reported previously [33-35]. According

to the ratio of signal to noise which equalled to 3, the limit of the detection was calculated to be 5 ppt, which was remarkably lower than that (0.3 ppb) of the electrode modified polyviologen for 5 min deposition through the stripping analysis [36] as well as those reported with the electrodes modified with Au NPs [37]. Table 1 shows the comparison result of our proposed sensor with other Hg(II) sensors.

Table 1. Comparison of our proposed electrochemical Hg(II) sensor with other reported sensors.

Electrode	Detection species	Linear detection range (ppn)	Limit of detection (ppb)	Reference
Activated graphite	Hg ²⁺	0.5-40	0.01	[38]
Bis(indolyl)methane/mesoporous carbon nanofiber/nafion	Hg ²⁺	3-60	0.05	[39]
Nanoporous gold nanoparticles	Hg ²⁺	0.1-17	0.03	[40]
MC-900	Hg ²⁺	0.005-50	—	This work

Due to the presence of other metal ions in the real samples, to detect Hg (II) with selectivity is a challenging. Especially, under the experimental condition employed in detecting Hg (II), these ions could be deposited together and stripped off. To assess the selectivity of the Au NPs-chi-graphene/GCE for the detection of Hg (II), the possible interferences induced by Cd (II), Fe (III), Cu (II) and Zn (II) ions were taken in account. The electrochemical stripping signals of mercury in the solution with 20 times of each element compared to Hg (II) were illustrated in Figure 6. It was obvious that the stripping peak current of Hg (II) with a concentration of 1.0 ppb changed slightly, which indicated that a negligible interfere of these metal ions was observed for the detection of mercury. Thus, MC-900/CGE could enhance the selectivity of the sensor significantly.

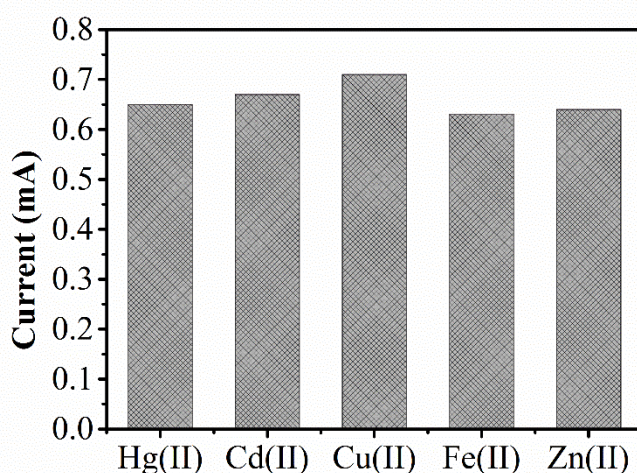


Figure 6. The influences of diverse metal ions on the electrochemical stripping signals of Hg²⁺ at MC-900/GCE (the content of Hg²⁺ is 1.0 ppb, where the content of Cd²⁺, Co²⁺, Cu²⁺, Fe³⁺, Zn²⁺, I⁻ was 20 ppb for each). Conditions: 0.1 M HCl; frequency: 40 Hz; amplitude: 20 Mv; potential increment: 4 mV.

Moreover, ten different electrodes were employed to evaluate the reproducibility of the MC-900/GCE. The relative standard deviation (R.S.D) of Hg (II) with a content of 10 ppb was calculated to be 4.32%, which indicated that the reproducibility was acceptable. Besides, the stripping response of mercury exhibited negligible decrease during the storage of the electrode at 4 °C for one week under dry condition. In particular, the sensor also remained 77% of the original current response after being stored for 30 days.

Table 2. Detection of Hg (II) in practical specimens with the designed MC-900/GC. Conditions: 0.1 M HCl; frequency: 40 Hz; amplitude: 20 Mv; potential increment: 4 mV.

Sample	Added (ppb)	Found (ppb)	ICP-MS result (ppb)	RSD (%)	Recovery (%)
1	0	0.48	0.45	4.55	—
2	0.5	0.97	0.96	3.67	98.98
3	1	1.47	1.51	7.84	99.32
4	1.5	2.02	2.01	3.31	102.02
5	2	2.57	2.55	4.51	103.63

Furthermore, the proposed electrode was used to analyze the river water specimens to confirm its practicality. In prior to the measurements, all the water specimens were spiked by Hg (II) with various concentrations. In Table 2, the initial concentration of the mercury in the river water specimen was measured to be 0.48 ppb, which was remarkably under the guideline value of Hg (II) (1 ppb) set by WHO for the drinking water. Besides, the accuracy of the proposed approach was also assessed through the comparison of the electrochemical results with those obtained with ICP-MS, where the result obtained with ICP-MS was 0.45 ppb. Only 6.9 % deviation was observed with these two approaches, which indicated that the proposed approach exhibited remarkable accuracy and precision and practicality for the direct analysis of the corresponding real specimens.

4. CONCLUSIONS

In conclusion, a facile route in the absence of any catalysts was employed to prepare carbon microspheres (MC-900) in large scale, where low-cost starting materials were used. Subsequently, the as-obtained MC-900 was succeeded to construct a new platform with remarkable performance towards the stripping analysis of Hg (II). Moreover, the as-constructed biosensor displayed an outstanding applicability in detecting Hg (II) involving in the real water specimens.

References

1. K.V. Gopal, *Neurotoxicology and teratology*, 25 (2003) 69.
2. L. Ebdon, M.E. Foulkes, S. Le Roux and R. Muñoz-Olivas, *The Analyst*, 127 (2002) 1108.
3. A. Iwashita, T. Nakajima, H. Takanashi, A. Ohki, Y. Fujita and T. Yamashita, *Talanta*, 71 (2007) 251.
4. S.R. Segade and J.F. Tyson, *Talanta*, 71 (2007) 1696.

5. Y. Zhang and S.B. Adeloju, *Talanta*, 74 (2008) 951.
6. W. Van Delft and G. Vos, *Anal. Chim. Acta.*, 209 (1988) 147.
7. E. Viltchinskaia, L. Zeigman, D. Garcia and P. Santos, *Electroanalysis*, 9 (1997) 633.
8. V.K. Gupta, *CHIMIA International Journal for Chemistry*, 59 (2005) 209.
9. A.K. Singh, V. Gupta and B. Gupta, *Anal. Chim. Acta.*, 585 (2007) 171.
10. A. Jain, V. Gupta, L. Singh and J. Raison, *Electrochimica Acta*, 51 (2006) 2547.
11. V.K. Gupta, R.N. Goyal and R.A. Sharma, *Talanta*, 78 (2009) 484.
12. V. Gupta and S. Agarwal, *Talanta*, 65 (2005) 730.
13. R. Prasad, V.K. Gupta and A. Kumar, *Anal. Chim. Acta.*, 508 (2004) 61.
14. Y. Zheng, A. Wang, W. Cai, Z. Wang, F. Peng, Z. Liu and L. Fu, *Enzyme and Microbial Technology*, (2016)
15. C. Brasquet and P. Le Cloirec, *Carbon*, 35 (1997) 1307.
16. L. Fu and A. Yu, *Rev. Adv. Mater. Sci*, 36 (2014) 40.
17. B. Crittenden, A. Patton, C. Jouin, S. Perera, S. Tennison and J.A.B. Echevarria, *Adsorption*, 11 (2005) 537.
18. M. Inagaki, *New Carbon Materials*, 24 (2009) 193.
19. Z. Liu, L. Ling, W. Qiao and L. Liu, *Carbon*, 37 (1999) 2063.
20. W. Qin, X.-Y. Liang, R. Zhang, C.-J. Liu, X.-J. Liu, W.-M. Qiao, Z. Liang and L.-c. LING, *New Carbon Materials*, 24 (2009) 55.
21. L. Fu, G. Lai, D. Zhu, B. Jia, F. Malherbe and A. Yu, *ChemCatChem*, 8 (2016) 2975.
22. S. Yenisoy-Karakaş, A. Aygün, M. Güneş and E. Tahtasakal, *Carbon*, 42 (2004) 477.
23. A. Romero-Anaya, M. Lillo-Ródenas and A. Linares-Solano, *Carbon*, 48 (2010) 2625.
24. B. Böhringer, O. Guerra Gonzalez, I. Eckle, M. Müller, J.M. Giebelhausen, C. Schrage and S. Fichtner, *Chemie Ingenieur Technik*, 83 (2011) 53.
25. A. Kurniawan, C. Effendi, L. Ong, F. Kurniawan, C. Lin, A.E. Angkawijaya, Y.-H. Ju, S. Ismadji and X. Zhao, *Electrochimica Acta*, 111 (2013) 99.
26. C. Wang, Y. Zhou, L. Sun, P. Wan, X. Zhang and J. Qiu, *Journal of Power Sources*, 239 (2013) 81.
27. J. Wang, L. Shen, B. Ding, P. Nie, H. Deng, H. Dou and X. Zhang, *RSC Advances*, 4 (2014) 7538.
28. Y. Fan, X. Yang, B. Zhu, P.-F. Liu and H.-T. Lu, *Journal of Power Sources*, 268 (2014) 584.
29. A. Cuesta, P. Dhamelincourt, J. Laureyns, A. Martinez-Alonso and J.D. Tascón, *Carbon*, 32 (1994) 1523.
30. H. Liu, X. Zhou, F. Wang, J. Ji, J. Liu, Z. Li and Y. Jia, *Mater. Res. Bull.*, 57 (2014) 280.
31. Y. Zhao, M. Liu, X. Deng, L. Miao, P.K. Tripathi, X. Ma, D. Zhu, Z. Xu, Z. Hao and L. Gan, *Electrochimica Acta*, 153 (2015) 448.
32. X. Wang, J. Guo, X. Yang and B. Xu, *Mater. Chem. Phys.*, 113 (2009) 821.
33. X. Dai, G.G. Wildgoose, C. Salter, A. Crossley and R.G. Compton, *Anal. Chem.*, 78 (2006) 6102.
34. O. Abollino, A. Giacomino, M. Malandrino, G. Piscionieri and E. Mentasti, *Electroanalysis*, 20 (2008) 75.
35. B. Kumar Jena and C. Retna Raj, *Anal. Chem.*, 80 (2008) 4836.
36. K.C. Cheng and P.Y. Chen, *Electroanalysis*, 20 (2008) 207.
37. H. Xu, L. Zeng, S. Xing, G. Shi, Y. Xian and L. Jin, *Electrochemistry Communications*, 10 (2008) 1839.
38. S. Palanisamy, R. Madhu, S.-M. Chen and S.K. Ramaraj, *Analytical Methods*, 6 (2014) 8368.
39. Y. Liao, Q. Li, N. Wang and S. Shao, *Sensors and Actuators B: Chemical*, 215 (2015) 592.
40. Y. Lin, Y. Peng and J. Di, *Sensors and Actuators B: Chemical*, 220 (2015) 1086.